THE JOURNAL OF PHYSICAL CHEMISTRY B

Article

pubs.acs.org/JPCB

Analyte Interactions with a New Ditopic Dansylamide–Nitrobenzoxadiazole Dyad: A Combined Photophysical, NMR, and Theoretical (DFT) Study

Abhas Kumar Bhoi,[†] Sudhir Kumar Das,[†] Debashis Majhi,[†] Prabhat Kumar Sahu,[†] A. Nijamudheen,[†,§] Anoop N.,[‡] Abdur Rahaman,[‡] and Moloy Sarkar*[,†]

[†]School of Chemical Sciences and [‡]School of Biological Sciences, National Institute of Science Education and Research, Bhubaneswar 751005, India

Supporting Information

ABSTRACT: We report herein the synthesis and photophysical studies on a new multicomponent chemosensor dyad comprising two fluorescing units, dansylamide (DANS) and nitrobenzoxadiazole (NBD). The system has been developed to investigate receptor–analyte binding interactions in the presence of both cations and anions in a single molecular system. A dimethyl amino (in the DANS unit) group is used as a receptor for cations, and acidic hydrogens of sulfonamide and the NBD group are used as receptors for anions. The system is characterized by conventional analytical techniques.

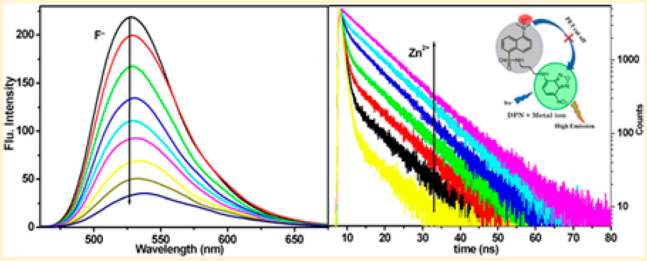

The photophysical properties of this supramolecular system in the absence and presence of various metal ions and nonmetal ions as additives are investigated in an acetonitrile medium. Utility of this system in an aqueous medium has also been demonstrated. The absorption and fluorescence spectrum of the molecular system consists of a broad band typical of an intramolecular charge-transfer (ICT) transition. A low quantum yield and lifetime of the NBD moiety in the present dyad indicates photoinduced electron transfer (PET) between DANS and the NBD moiety. The fluorescence intensity of the system is found to decrease in the presence of fluoride and acetate anions; however, the quenching is found to be much higher for fluoride. This quenching behavior is attributed to the enhanced PET from the anion receptor to the fluorophore moiety. The mechanistic aspect of the fluoride ion signaling behavior has also been studied by infrared (IR) and ^{1}H NMR experiments. The hydrogen bonding interaction between the acidic NH protons of the DPN moiety and F^- is found to be primarily responsible for the fluoride selective signaling behavior. While investigating the cation signaling behavior, contrary to anions, significant fluorescence enhancement has been observed only in the presence of transition-metal ions. This behavior is rationalized by considering the disruption of PET communication between DANS and the NBD moiety due to transition-metal ion binding. Theoretical (density functional theory) studies are also performed for the better understanding of the receptor–analyte interaction. Interestingly, negative cooperativity in binding is observed when the interaction of this system is studied in the presence of both Zn^{2+} and F^-. Fluorescence microscopy studies also revealed that the newly developed fluorescent sensor system can be employed as an imaging probe in live cells.

1. INTRODUCTION

The design and synthesis of fluorescent sensors for detection of metal ions as well as nonmetal ions have attracted considerable attention in recent times.[1−12] The enthusiasm in this field originates from the important role played by metals and nonmetal ions in biomedical, environmental, and industrial fields.[1] Examples of such sensor molecules or arrays of molecules have been constructed from organic chromophores/lumophores, inorganic–metal frameworks, coordination frameworks, or the suitable combination of any of these.[1−12] This gives rise to rich varieties of structural motifs where sensing by optical means can be stimulated by light energy, for example, by direct excitation or via electron-transfer or energy-transfer processes in donor–acceptor arrays or electrochemical or chemical inputs such as ions or neutral molecules.[1−12] For recognition and detection of anions, hydrogen bonding interactions are mainly exploited. Most of the neutral anion sensors employ polarized N–H fragments for anion recognition and are based upon ureas, thioureas, amides, amidoureas, pyrroles, and amines in aprotic solvents.[9] A recent report demonstrated that structural modifications in the (thio)urea moiety are helpful in achieving better anion binding.[12] The recognition phenomenon in these examples normally involves noncovalent interactions such as either H-bonding (partial proton transfer) or complete deprotonation of N–H protons.[5−12] The significance of such noncovalent

Received: May 11, 2014
Revised: July 23, 2014
Published: August 4, 2014

   dx.doi.org/10.1021/jp504631n | J. Phys. Chem. B 2014, 118, 9926–9937

interactions lies in their ability to be formed as well as broken easily without use of much energy.[13] On the other hand, detection of cations by exploiting suitable supramolecular systems has been achieved by exploiting processes like photoinduced electron transfer (PET),[3] resonance energy transfer (RET),[14] and excimer formation.[15] Many structures based on simple amines, cryptands, crown ethers, calixarenes, podands, and peptides have been used as receptor moieties for this purpose.[16−20] The strategies behind all of these receptors is to have much weaker metal−fluorophore (M−F) communication while at the same time having much stronger metal−receptor (M−R) interaction.[21] Sensing via optical means has gathered more attention as compared to classical methodologies mainly because of its ability to monitor in situ analyte concentrations in real time and, eventually, in real space. Fluorescence, in particular, is quite advantageous and superior because of its very high sensitivity (detection at the single-molecule level is also possible now[22]).

Despite the fact that several molecular systems were designed and developed for the detection of either cations or anions, a molecular system that can act as a sensor for anions and cations in a single molecular system remains rather limited.[22−28] Interestingly, these ditopic receptors could also exhibit cooperative effects, where the binding of one ion affects the binding affinity of other.[25,26] The complexity in the structure of such a supramolecular system required for simultaneous detection of cations and anions has often made their synthesis a difficult task. Thus, it is very desirable to develop a simple targeted molecular system that can simultaneously detect both cations and anions. In this regard, a proper knowledge about the receptor−analyte interaction will be helpful in designing a chemosensor for specific analytes. Even though several experimental reports are available on molecular recognition, theoretical studies[29−36] on these aspects are rather limited.

Herein, we report the design and synthesis of a molecular system (DPN, Chart 1) for detecting certain metal ions and nonmetal ions. DPN is developed by combinig 7-nitrobenz-2-oxa-1, 3-diazole (NBD), and 5-(dimethylamino)naphthalene-1-sulfonylamide (dansylamide) fluorophores (electron donor) due to their suitable photophysical[37−39] and biological[40−42] properties.

Chart 1. Molecular Structure of the Target Molecule DPN and Parent Fluorophore NBDP

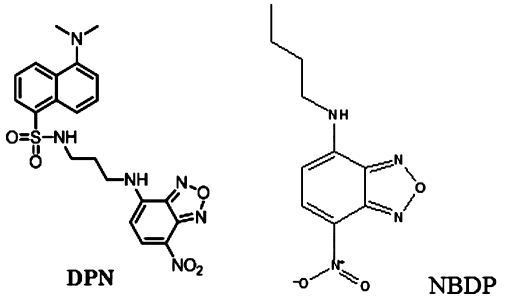

The target molecule (DPN) is designed based on the [receptor (cation)−spacer−receptor (anion)−fluorophore] architecture (Chart 1). Whereas the dimethylamino group of the dansylamide group is used for cation binding (coordination with a N atom lone pair), the propyl group acts as the spacer unit, and acidic hydrogens of sulfonamide and the NBD group are used for the receptor (H-bonding interaction). We have also prepared 4-butylamino-7-nitro-2,1,3-benzoxadiazole (NBDP)[35] to compare the fluorescence yield and lifetime of NBDP to that of the present system (DPN). The systems are shown in Chart 1.

The system is designed in such a way that binding of anions and cations to their corresponding receptors results in the alteration of charge transfer (through-bond or through-space) between the fluorophore and receptors. These binding events are monitored in acetonitrile (ACN) through changes in the absorbance and fluorescence response upon binding of anions and cations. The photophysical behavior in the absence and presence of various cations and anions has been studied by steady-state and time-resolved fluorescence experiments as well as by NMR and theoretical studies. The outcome of the present combined experimental and theoretical study of the receptor−analyte interaction would be helpful to understand the subtleties of the signaling mechanism and consequently designing an efficient chemosensor for the analyte of interest.

2. EXPERIMENTAL SECTION

2.1. Materials. Dansyl chloride, 1,3-diaminopropane, and 4-chloro-7-nitrobenzoxadiazole were purchased from Sigma−Aldrich. In the titration experiments, all anions, in the form of tetrabutyl ammonium (TBA) salts, and all cations, in the form of perchlorate salts, were purchased from Sigma−Aldrich. Solvents used for the synthesis were received from Sigma−Aldrich. For the titration purposes, solvents were dried and distilled by published procedures.[43] Deutrated chloroform ($CDCl_3$) and dimethyl sulfoxide [$(CD_3)_2SO$] (Sigma−Aldrich) were used for NMR titrations.

2.2. Instrumentation. ^{1}H NMR spectra were obtained on a Bruker biospin 400 MHz spectrometer at ambient temperature using tetramethylsilane (TMS) as an internal standard. The same setup was used for ^{1}H titrations. UV/vis and fluorescent spectra were recorded using a PerkinElmer Lambda 750 UV/vis spectrometer and a PerkinElmer LS-55 fluorescence spectrophotometer. A PerkinElmer FTIR spectrometer (Spectrum RXI) was used to record IR spectra. Time-resolved fluorescence measurements were carried out by using a time-correlated single-photon counting (TCSPC) spectrometer (Edinburgh, OB920). A diode laser ($\lambda_{exc.}$ = 405 nm, full width at half-maxima (fwhm) ≈ 95 ps) was used to excite the molecules, and a microchannel plate (MCP) photomultiplier (Hamamatsu R3809U-50) was used as the detector (response time 40 ps). The source profile was recorded by using a scatterer (dilute Ludox collidal dispersion in water) in place of the sample. Decay curves were analyzed by a nonlinear least-squares iteration procedure using the F900 decay analysis software. Global analysis of the decay profiles was carried out by using the FAST program package (Edinburgh). The quality of the fit was judged by the chi squared (χ^2) values, and weighted deviations were obtained by fitting.

2.3. Fluorescence Quantum Yield Measurement. For quantum yield measurements, optically matched solutions (at the excitation wavelength) were used. The quantum yield was calculated by measuring the integrated area under the emission curves and by using eq 1[44]

$$\phi_{sample} = \frac{I_{sample} \times OD_{standard} \times \eta^2_{sample}}{I_{standard} \times OD_{sample} \times \eta^2_{standard}} \times \phi_{standard} \quad (1)$$

where ϕ is the quantum yield, I the integrated emission intensity, OD the optical density at the excitation wavelength,

dx.doi.org/10.1021/jp504631n | J. Phys. Chem. B 2014, 118, 9926−9937

Scheme 1. Synthetic Route to DPN

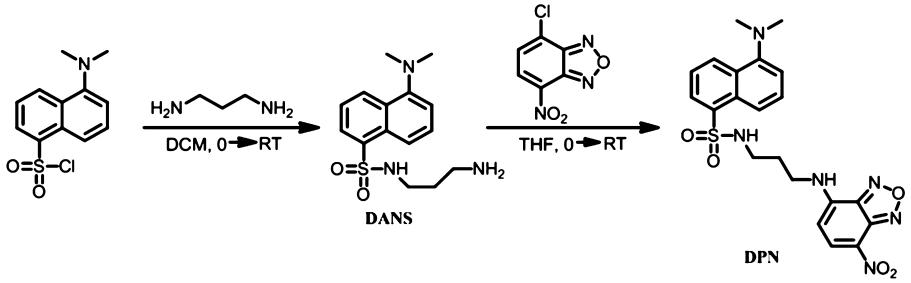

and η the refractive index. Fluorescence quantum yields of DPN were measured using coumarin 153 (in ACN, $\phi = 0.89$)[45] as the standard.

2.4. Computational Methods. The ground-state structures were optimized using the hybrid density functional M06-2X[46,47] and 6-31+G(d)[48] and LANL2DZ (metal) basis sets.[49] All positive vibrational frequencies obtained at the same level of theory ensure that the located geometries represent true minima. Single-point energies were then computed using triple-ζ quality basis sets 6-311++G(d,p) and LANL08 (metal ions).[50] Hence, all of the interaction energies reported here are from M06-2X/6-311++G(d,p), LANL08(metal ions)//M06-2X/6-31+G(d), and LANL2DZ (metal ions) levels of theory unless specified otherwise. Interaction energies of DPN−metal ion complexes (DPN···M^{n+}) were calculated as $\Delta E_{int} = E_{(DPN\cdots M^{n+})} - E_{(DPN)} - E_{M^{n+}}$, where $E_{(DPN\cdots M^{n+})}$, $E_{(DPN)}$, and $E_{M^{n+}}$ represent the energy of the metal complex, DPN, and metal ion, respectively. In order to account for the basis set superposition errors (BSSEs), a counterpoise correction scheme was applied.[51] Time-dependent density functional theory (TDDFT) calculations were carried out at the B3LYP level of theory[52] employing 6-311++G(d,p) and LANL08 (Zn) basis sets and an implicit solvation model[53] for ACN to understand the excited-state properties of DPN and the DPN···Zn^{2+} complex. All of the calculations were carried out using the Gaussian 09 suite of programs.[54]

2.5. Binding Constant Evaluation from Fluorescence Titration. The binding constants for analytes were also determined from the fluorescence data by using the Benesi−Hildebrand plot.[55]

2.6. Synthesis of Molecular Systems. *Synthesis of 3-Aminopropyldansylamide (DANS) (Scheme 1).* To a solution of 1,3-diaminopropane (2.468 g, 33.364 mmol) in dichloromethane (DCM, 25 mL) was added dansyl chloride (200 mg, 0.74 mmol) in DCM (20 mL) dropwise at 0 °C, and the reaction was allowed to proceed with stirring for 1 h when the solution gradually attained room temperature. The reaction mixture was then extracted with 1 M aqueous hydrochloric acid (HCl, 3 × 50 mL). The aqueous phase was basified with a 5 M sodium hydroxide (NaOH) solution. Again, the aqueous phase was extracted with DCM. The collected organic phase was dried over anhydrous sodium sulfate (Na_2SO_4), and the organic phase then evaporated under reduced pressure to obtain a yellowish-white product (DANS). Yield = 200 mg (88%). The compound was characterized by ^{1}H NMR and mass spectrometry.

^{1}H NMR ($CDCl_3$): 8.53 (d, 1H), 8.31 (d, 1H), 8.25 (d, 1H), 7.59 (d, 1H), 7.52 (d, 1H), 7.18 (d, 1H), 3.01 (t, 2H), 2.89 (s, 6H), 2.69 (t, 2H), and 1.48 ppm (p, 2H). ESI-MS: 308.14 ($M+H^+$).

Synthesis of DPN (Scheme 1). 4-Chloro-7-nitrobenzoxadiazole (108 mg, 0.542 mmol) in dry tetrahydrofuran (THF) (20 mL) was added to a solution of DANS (200 mg, 0.65 mmol) dissolved in 20 mL of dry THF at 0 °C. The mixture was stirred under an argon atmosphere for 1 h (0 °C to room temperature) and for another 3 h at room temperature. The reaction mixture was evaporated under reduced pressure to obtain a reddish-black crude product. The residue was further purified by column chromatography on silica gel (ethyl acetate/hexane = 1:4 initially for better separation and then ethyl acetate/hexane = 10:1 to elute down the product) to provide a red solid DPN (210 mg, 0.503 mmol, 82.4%). The compound was characterized by ^{1}H NMR and mass spectrometry.

^{1}H NMR ($CDCl_3$): 8.54 (d, 1H), 8.40 (d, 1H), 8.29 (t, 2H), 7.60 (d, 1H), 7.55 (d, 1H), 7.20 (d, 1H), 6.63 (s, 1H), 5.99 (d, 1H), 5.06 (d, 1H), 3.60 (q, 2H), 3.08 (q, 2 H), 2.90 (s, 6H), and 1.92 ppm (p, 2H). ESI-MS: 471.14 ($M+H^+$).

3. RESULTS AND DISCUSSION

3.1. Molecular Design and Synthesis. The design of the target molecule (DPN) is based on a [receptor (cation)−spacer−receptor (anion)−fluorophore] architecture. The nitrobenzoxadiazole moiety is purposefully used as the main fluorescing moiety primarily because of its high fluorescence quantum yield and electron-deficient nature.[37] The propyl spacer with one end having a sulfonamide moiety and the other end with an amine moiety is expected to be responsible for the binding interaction with anions. These N−H protons of the NBD group and dansylamide moiety are polarizable and thus can participate in hydrogen bonding interactions with anions.[9] The pK_a values corresponding to the acidic sulfonamide hydrogen of the dansylamide moiety and the NH proton of the HNBD moiety are reported to be 6.23[56] and 12,[32] respectively, in aqueous medium. In the molecular assembly, the dimethyl amino group serves as the receptor for metal ions.

3.2. Photophysical Behavior of DPN. The absorption and emission behavior of DPN have been investigated as a function of solvent polarity. Figure 1 shows the representative absorption and emission spectra of DPN in ACN. Spectral data corresponding to absorption and emission maxima of DPN in several solvents are presented in Table 1. Free DPN shows a broad absorption band with a peak at 460 nm and a broad fluorescence band with a maximum at 531 nm in ACN (Figure 1). Upon increasing the polarity of the medium from toluene to ACN, a bathochromic shift of both the absorption and emission maxima is observed (Table 1). For example, a bathochromic shift of the absorption band of 12 nm is observed upon changing the solvent from apolar toluene to polar ACN. From these solvatochromic responses of the DPN molecule, one can conclude that the broad absorption and emission band of the

dx.doi.org/10.1021/jp504631n | J. Phys. Chem. B 2014, 118, 9926−9937

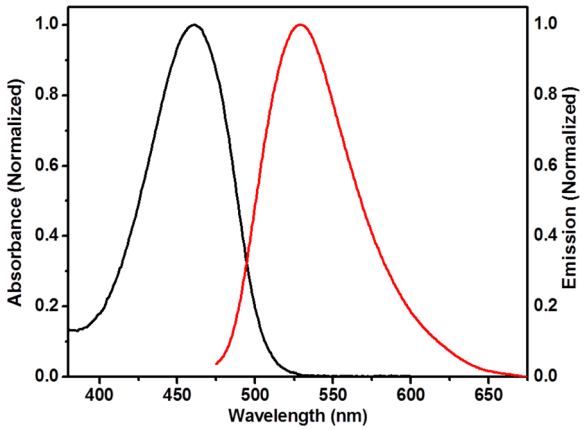

Figure 1. Absorption and emission spectra of DPN in ACN. All spectra are normalized at their corresponding peak maxima. $\lambda_{exc.}$ = 460 nm.

Table 1. Absorption and Fluorescence Spectral Data of DPN in Toluene, THF, and ACN in nm

	toluene (33.6)[a]	THF (37.4)[a]	ACN (45.6)[a]
λ_{max}^{abs}	448	457	460
λ_{max}^{flu}	509	520	529

[a]Quantities in the parentheses indicate the micropolarity parameter [$E_T(30)$] values of the solvents.

present system is due to the intramolecular charge-transfer (ICT) transition from amino nitrogen to the nitro group of the NBD moiety. Emission from other NBD−amine systems is known to occur from the ICT state.[32]

The fluorescence quantum yield of DPN in ACN medium measured from the steady-state emission spectra is found to be 0.065 (using coumarin 153 as the standard, ϕ_{std} = 0.89 in ACN[45]). This value is quite less as compared to the fluorescence quantum yield (0.74) of the parent fluorophore (NBDP).[32] The 91% decrease in fluorescence quantum yield is attributed to the PET from the electron-rich receptor moiety (dimethyl amino group of DANS) to the NBD moiety of the DPN system.

In order to get a better idea about the PET mechanism, the time-resolved fluorescence decay behavior of DPN has also been investigated in an ACN medium. While measuring the fluorescence decay behavior, DPN is excited at 445 nm, and its emission is monitored at 530 nm. It may be mentioned that 530 nm emissions correspond to that of the NBD moiety only. The time-resolved emission decay profile of DPN is shown in Figure 2. The decay profile is fitted to a biexponential function [τ_1 = 0.89 ns (98%), τ_2 = 8.66 ns (2%)]. The average lifetime is found to be 1.04 ns. The fluorescence decay behavior of its parent molecule (NBDP) is reported to be a single exponential with a lifetime of 10.2 ns in the ACN medium.[35] The short-lived component generally represents the lifetime of the species where the donor and acceptor groups are in PET communication.[37] The short-lived component in the present case clearly represents a PET-quenched fluorophore where PET occurs from the dimethylamine (donor) to nitro-benzoxadiazole (acceptor) moiety. The long-lived minor component may, in principle, arise from the species where donor and acceptor groups are not in close proximity.[37] The rate of the PET process in the ACN medium is estimated by using the following relation[57]

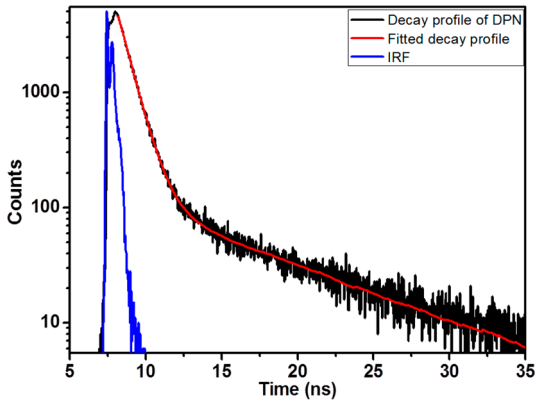

Figure 2. Fluorescence decay curve of DPN in ACN. $\lambda_{exc.}$ = 445 nm.

$$\langle k_{ET} \rangle = \frac{1}{\langle \tau_{DPN} \rangle} - \frac{1}{\langle \tau_{NBDP} \rangle} \quad (2)$$

In the present case, $\langle k_{ET} \rangle$ in an ACN medium is estimated to be 8.63 ($\times 10^9$ s^{1-}). It may be mentioned in this context that no rise time (growth component) is observed while monitoring NBD emission. This observation clearly rules out the possibility of RET between dansylamide and the NBD moiety.

The thermodynamic feasibility of PET between the dimethylamino group of dansylamide (donor) and the NBD (acceptor) fluorophore has also been verified. The fact that PET in the present system is thermodynamically feasible becomes evident when we monitor the spectral behavior of DPN along with oxidation and reduction potential values of donor and acceptor moieties. The reduction potential (E_{red}) value of the acceptor fluorophore (NBD) is reported to be −0.91 eV,[37] whereas the oxidation potential (E_{ox}) of the donor (dansylamide) is reported to be 0.94 eV.[58] The singlet-state energy of the fluorophore ($E_{0,0}$) is estimated to be 2.51 eV. Thus, the free-energy change (ΔG^*) for the PET process, calculated by Weller's equation, is $\Delta G^* = E_{ox}(\text{receptor}) - E_{red}(\text{fluorophore}) - E_{0,0} - q_1q_2/4\pi\varepsilon_0\varepsilon_s r = 0.94 - - 0.91 - 2.51 - 0.033 = -0.69$ eV. Here, ε_0, ε_s, and r are the permittivity of the vacuum, the dielectric constant of the solvent, and the donor−acceptor distance (1.211 nm). q_1 and q_2 are the charges of donor and acceptor centers, respectively. The observation of a negative value of the free-energy change provides evidence in favor of the thermodynamic feasibility of PET between the dimethylamino group of dansylamide (donor) and the NBD (acceptor) fluorophore.

3.3. Interaction of Anions with DPN. The fluorophore−analyte interaction with various biologically important anions has been investigated following spectrophotometric as well as fluorometric titration experiments in an ACN medium. All titrations have been carried out by adding freshly prepared tetrabutlyammonium salts of the corresponding anion ($\sim 10^{-5}$ M) to the dilute solution of DPN ($\sim 10^{-6}$ M) in a stepwise fashion. In particular, upon progressive addition of fluoride salt, a new band at ∼395 nm is developed (Figure 3). We have earlier shown that the ∼395 nm band can arise due to the formation of a receptor−F^- complex through hydrogen bonding interactions between the NH proton of the NBD moiety and fluoride.[32] Fluoride being a strong electronegative ion could easily form a H-bond complex with the acidic NH protons. It may be mentioned in this context that because the N−H proton (SO_2NH) of the dansylamide moiety is also polarizable and acidic in nature, it can participate in hydrogen

dx.doi.org/10.1021/jp504631n | J. Phys. Chem. B 2014, 118, 9926−9937

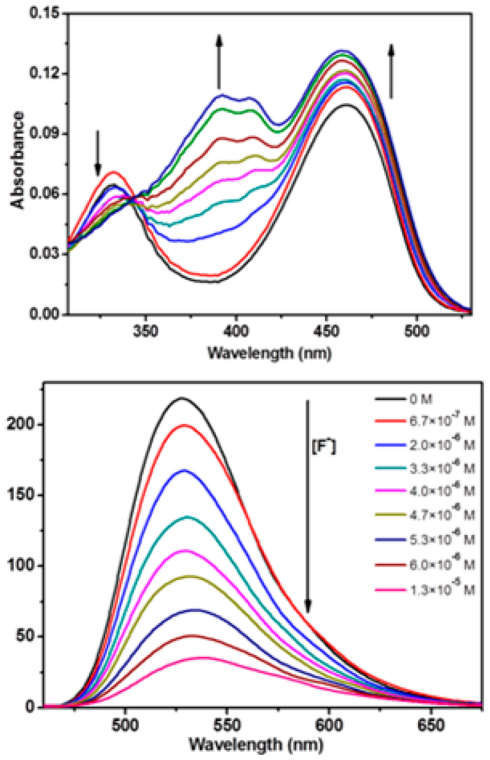

Figure 3. Absorption (upper panel) and emission (lower panel) spectra of DPN (1.5×10^{-6} M) in ACN upon progressive addition of TBAF. The concentration of TBAF in various solutions ranges from 0 to 1.3×10^{-5} M.

bonding interactions with fluoride anions. However, because SO_2NH is not in conjugation with the NBD moiety, a change in the absorption spectrum due to binding of F^- to this site is not expected.

Upon gradual addition of F^- to the solution of DPN, a significant decrease in intensity of the 527 nm fluorescence band takes place (Figure 3). In this context, the variation of the quantum yield of DPN with the addition of a fluoride ion has been provided in the Supporting Information (Figure S1). The variation of the relative fluorescence intensity of DPN with and without addition of fluoride is also shown in Figure S2 (Supporting Information). The monotonous decrease in emission intensity of DPN upon addition of F^- in the steady-state emission spectrum indicates that the receptor–F^- complex is nonfluorescent in nature. The NBD–F^- complex is known to be nonfluorescent.[32] However, because a new receptor–F^- complex can also be formed between the acidic hydrogen (SO_2NH) of dansylamide and fluoride, we would like to stress that the quenching process may also be augmented by the increase in PET from the receptor (SO_2NH) to the fluorophore (NBD) moiety due to hydrogen bonding. Hydrogen bonding interactions increase the reduction potential of the receptor, which in turn makes the PET from the receptor to the fluorophore more favorable.[3]

To test the selective behavior of the present system, we have carried out similar experiments with other commonly encountered anions by UV/vis absorption and fluorescence titration measurements. The system did not show any significant changes in the fluorescence intensity with other anions except the acetate ion, which showed some quencing effects in contrast to other anions. The selective behavior of the receptor toward fluoride is well understood when we plot the fluorescence responses of the system with the anions in a bar diagram (Scheme 2). The binding constants of DPN with F^-

Scheme 2. Bar Diagram Showing the Fluorescence Response of DPN to Selected Anions in ACN[a]

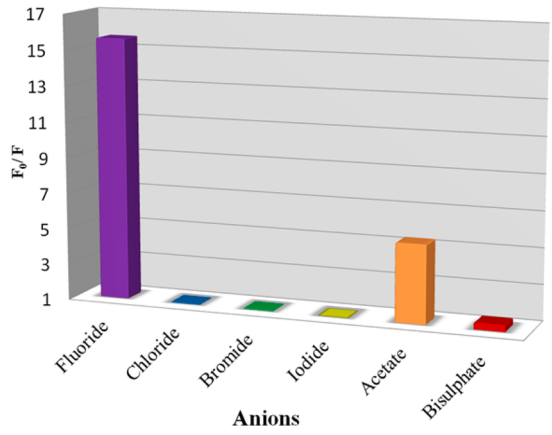

[a] F_0 stands for the fluorescence intensity of free molecules, and F stands for the fluorescence intensity in the presence of anions. Concentration are in the range of 0–7.6×10^{-5} M for each anions.

and acetate have been evaluated from fluorescence spectra using the Benesi–Hildebrand equation.[55] The binding constants were estimated to be 1.151×10^5 and 1.446×10^3 M^{-1} for F^- (Figure S4, Supporting Information) and acetate$^-$ ions, respectively. The binding constant for the fluoride ion was also estimated from the absorption data (Figure S3, Supporting Information). From the absorption data, the binding constant between DPN and F^- is calculated to be 3.24×10^5 M^{-1}. A relatively higher binding constant value for fluoride ions with DPN reflects the selectivity of the system toward F^-.

To investigate the DPN–anion interaction further, time-resolved fluorescence decay measurements (Figure 4) have also

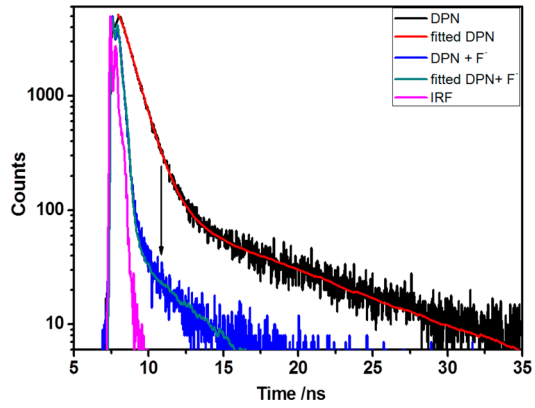

Figure 4. Fluorescence decay curve of DPN in ACN in the absence and presence fluoride ions. $\lambda_{exc.}$ = 445 nm.

been carried out in an ACN medium both in the presence and absence of fluoride and acetate ions. The average lifetimes of DPN are found to decrease with the addition of fluoride as well as acetate (Table 2). However, the decrease in lifetime in the presence of fluoride is found to be more than that of acetate. The significant drop in the fast component of the fluorescence lifetime due to addition of F^- perhaps indicates the enhancement in the PET process due to anion binding.

dx.doi.org/10.1021/jp504631n | J. Phys. Chem. B 2014, 118, 9926–9937

Table 2. Decay Parameters of DPN in the Absence and Presence of Fluoride and Acetate Ions

	a_1[a]	τ_1 (ns)[b]	a_2[a]	τ_2 (ns)[b]	a_3[a]	τ_3 (ns)[b]	τ_{avg} (ns)[b]	χ^2
DPN	0.98	0.89	0.02	8.66			1.04	1.18
DPN + F^-	0.99	0.13	0.01	3.68			0.16	0.92
DPN + AcO^-	0.46	0.15	0.07	1.43	0.47	6.92	0.38	0.91

[a] a_1, a_2, and a_3 are pre-exponential factors. [b] Lifetimes τ_1, τ_2, τ_3, and τ_{avg} are given in nanoseconds, and χ^2 are goodness-of-fit parameters.

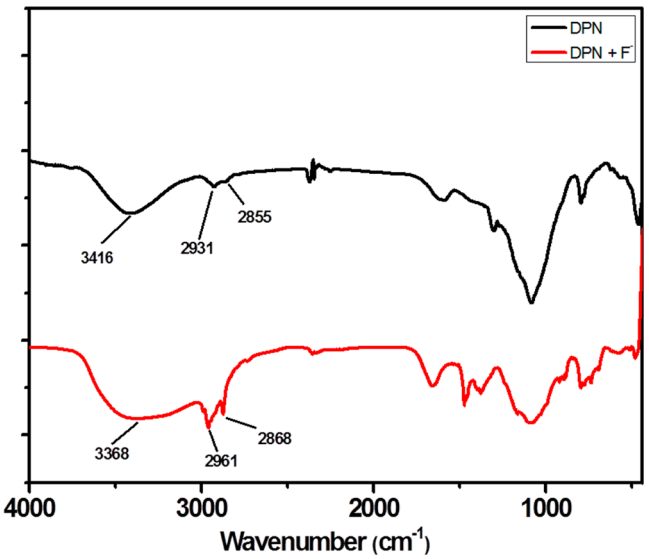

Figure 5. IR spectrum of DPN (black) and DPN in the presence of F^- salts (red).

To throw more light on the binding interactions of DPN with fluoride, we resorted to FTIR and NMR studies. Figure 5 represents the IR spectra of DPN in the absence and presence of F^-. It can be seen that the characteristic stretching for the N−H group for the DPN system that appears at 3416 cm^{-1} becomes broadened and appears at a lower energy (to that of free) in the presence of F^-. This broadening and decrease in vibrational frequency also supports the weakening of the N−H bond due to the hydrogen bonding interaction between F^- and the N−H proton.

In the NMR spectra (Figure 6), the N−H proton of the dansylamide group and the N−H proton corresponding to the NBD moiety appear at 9.25 and 6.02 ppm, respectively. Upon addition of F^-, the signal corresponding to the NH proton at 9.25 ppm gradually broadens with the concomitant loss of intensity. At a total 1.05 equiv. concentration of the F^- ion, the signal at 9.25 ppm is found to be significantly broadened and merged into the baseline (Figure 6), whereas no noticeable change in the N−H proton signal (6.02 ppm) of the NBD moiety has been observed. At this stage of F^- addition, no new NMR signal at ∼16 ppm is observed, which clearly rules out the possibility of formation of HF_2^- species[32] due to abstraction of an acidic proton by F^-. The observed NMR spectral changes caused by the receptor−fluoride hydrogen bonding in the present case are consistent with literature reports.[8,36]

3.4. Interaction of Cations with DPN. The interactions between DPN and metal ions in ACN have been investigated using UV/vis and fluorescence titration experiments. Spectrophotometric titrations have been performed on a dilute solution of DPN adding a freshly prepared metal perchlorate salt solution in a stepwise manner. Representative absorption and emission spectra of DPN in the absence and presence of Zn^{2+} ions are shown in Figure 7.

As can be seen from Figure 7, upon progressive addition of the metal salt, the lowest-energy absorption band that corresponds to the NBD moiety is not significantly affected, but the intensity of the absorption band at 332 nm is observed to be gradually decreased with the simultaneous formation of a new band at 286 nm. The observed spectroscopic response is a clear indication of binding of metal ions (Zn^{2+}) to the *N*,*N*-dimethylamino nitrogen atoms of the dansylamide group.[59] Interestingly, when DPN is excited at 445 nm (where a change in the absorbance corresponding to the NBD moiety due to metal ion additions is negligible), considerable fluorescence

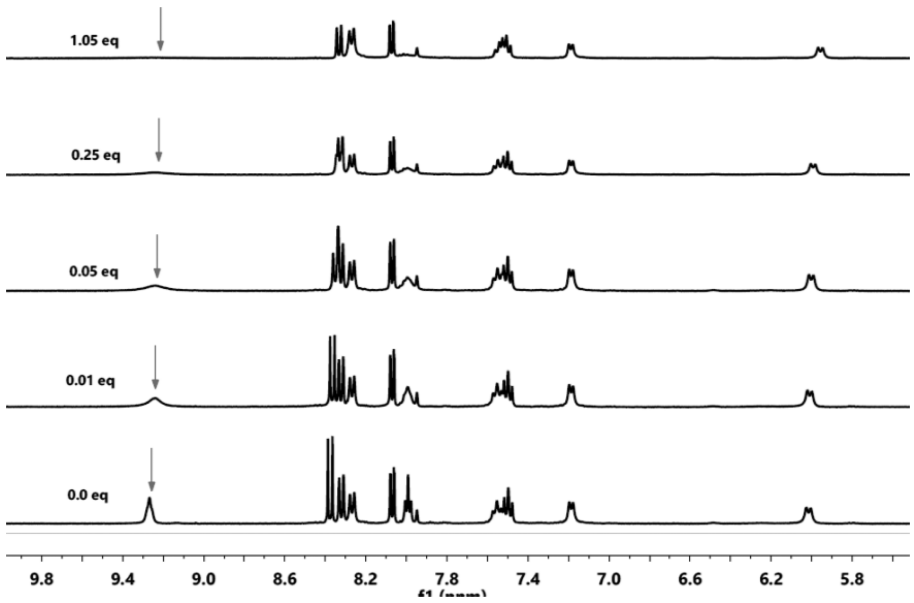

Figure 6. ^1H NMR spectra of DPN in DMSO-d_6 in the presence of different equivalents of TBAF.

dx.doi.org/10.1021/jp504631n | J. Phys. Chem. B 2014, 118, 9926−9937

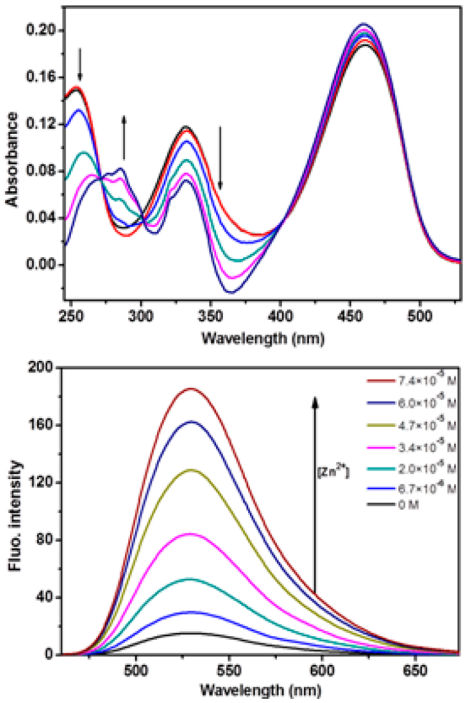

Figure 7. Absorption (upper panel) and emission (lower panel) spectra of DPN (~1.3 × 10^{-5} M) in ACN upon the progressive addition of $Zn(ClO_4)_2$. Concentrations of $Zn(ClO_4)_2$ in various solutions range from 0 to 9.33 × 10^{-5} M.

enhancement is observed (Figure 7). This is attributed to the disruption of PET communication between the cation receptor moiety (dimethylamine) and the fluorophore, as shown in Scheme 3. Lone electron pairs of the nitrogen atom of the dimethylamine group are utilized due to the binding of the metal ion to the receptor moiety, which in turn makes electron transfer from dimetyl amine to the fluorophore difficult.

Similarly, interactions of DPN in ACN with other cations, such as transition-metal ions and alkali and alkaline earth metals, have also been studied by UV/vis absorption and fluorescence titration measurements. Among these cations, transition- metal ions show significant (~12 times) fluorescence enhancement without appreciable change in absorbance. However, alkali and alkaline earth metal ions do not demonstrate any noticeable change in the emission of DPN. The fluorescence enhancement responses of different cations in ACN are provided in Figure S6 and compared in Scheme S1 (Supporting Information).

The binding constants of DPN with alkali and alkaline earth metals and transition-metal ions are calculated from fluorescence emission spectra using the Benesi−Hildebrand equation.[55] The binding constants for transition-metal ions are presented in Table 3. As can be seen from Table 3,

Table 3. Binding Constants for Transition-Metal Ions with DPN

transition-metal ions (M^{2+})	binding constant
Cu	45.36 × 10^4 $M^{-3/2}$ [a]
Zn	1.284 × 10^4 M^{-1} [b]
Pb	2.431 × 10^4 M^{-1} [b]
Cd	0.432 × 10^4 M^{-1} [b]
Mn	0.019 × 10^4 M^{-1} [b]
Fe	0.069 × 10^4 M^{-1} [b]

[a]2:3 binding [Cu_3(dansyl)$_2$]. [b]1:1 binding (other other metal ions).

copper(II) binds with strongest affinity with DPN followed by Zn^{2+}, Pb^{2+}, Cd^{2+}, and Cr^{3+}. The relative intensity plots also support the observed binding of the transition-metal ions except for Cu^{2+}, which shows deviation from its expected result (Scheme S1, Supporting Information). Interestingly, Cu^{2+} is known to form a stable 2:3 (ligand/metal ion) complex with dansylamide-based ligands where both dimethylamine and sulfonamide groups participate in bonding.[59] In the present case, similar complexation behavior is observed, and the stoichiometry (2:3) of the complex (DPN/Cu^{2+}) is confirmed via a Jobs plot (Figure S7, Supporting Information). Interestingly, the Jobs plot reveals a 1:1 stoichiometry of the complex between DPN and the Zn^{2+} ion (Figure S9, Supporting Information). The mode of binding between the ligand (DPN) and metals ions (Cu^{2+} and Zn^{2+}) is again verified by carrying out NMR experiments (vide infra). The unusual behavior for Cu^{2+} resulted from the anomalous binding with the dansylamide moiety.[59] It is pertinent to mention in this context that Cu^{2+} (paramagnetic) being the notorious quencher of fluorescence may also induce quenching of the fluorophore through M−F interaction.[21] Perhaps, because of these factors, the recovery of fluorescence upon binding of the Cu^{2+} ion with the DPN molecule is not as large as is observed for other transition-metal ions like Zn^{2+}. Zn^{2+} (diamagnetic) interacts only with the dimethylamino group (1:1 binding), leading to complete disruption of the PET process from dimethylamine to the fluorophore (NBD) taking place, which ultimately results in larger recovery of fluorescence of the fluorophore. To find out the suitability of the present system in practical applications, the interaction of the present system with Zn^{2+} has also been

Scheme 3. Schematic Diagram Illustrating Disruption of PET in the Presence of a Metal Ion

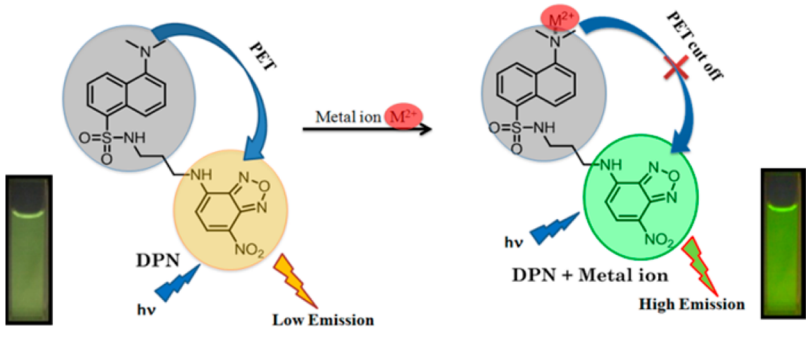

dx.doi.org/10.1021/jp504631n | J. Phys. Chem. B 2014, 118, 9926−9937

studied (Figure S10, Supporting Information) in ACN/H_2O (5:95, v/v).

To investigate the cation binding ability of DPN further, time-resolved fluorescence decay measurements (Figure 8) of

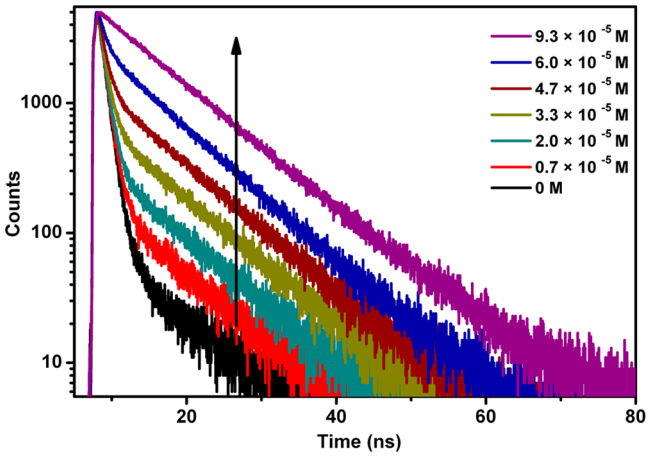

Figure 8. Fluorescence decay curve of DPN in ACN in the absence and presence of Zn^{2+}. The concentrations of Zn^{2+} in various solutions are provided. $\lambda_{exc.}$ = 445 nm.

the present system in both the absence and presence of Zn^{2+} and Cu^{2+} ions have been performed in an ACN medium. The average lifetime of DPN is observed to increase with the gradual addition of Zn^{2+} ion (Table 4). As can be seen from

Table 4. Decay Parameters and Average Lifetime of DPN in the Absence and Presence of Zn^{2+}

Zn^{2+} conc. ($\times 10^{-5}$ M)	a_1[b]	τ_1 (ns)[a]	a_2[b]	τ_2(ns)[a]	τ_{avg} (ns)[a]	χ^2
0.0	0.99	0.87	0.01	8.18	0.94	1.08
0.67	0.98	0.86	0.02	8.57	1.01	1.09
2.00	0.95	0.85	0.05	8.85	1.25	1.01
3.33	0.91	0.88	0.09	8.84	1.60	1.05
4.67	0.82	0.90	0.18	8.74	2.31	1.02
6.00	0.62	0.87	0.38	8.32	3.71	1.03
9.33			1.00	9.02	9.02	1.17

[a]Lifetimes τ_1, τ_2, and τ_{avg} are given in nanoseconds. [b]$a_1$and a_2 are pre-exponential factors, and χ^2 are the goodness-of-fit parameters.

Table 4 (last row), after the final addition of Zn^{2+}, the lifetime value of the system becomes comparable to the average lifetime value (10.2 ns) of the parent fluorophore. At the same time, one can clearly also observe from Figure 10 that the short component of the decay profile of DPN gradually vanishes, and the biexponential nature of the decay profile of DPN gradually changes to a single-exponential decay upon binding with the Zn^{2+} ion. This observation is a clear reflection of the disruption of the PET communication from the dimethyl amino moiety to the NBD moiety upon metal ion binding. More interestingly, unlike Zn^{2+}, at a relatively higher concentration of Cu^{2+} ions (Table 5, last two rows), the average lifetime of the fluorophore is observed to be decreased. As stated earlier, deSilva[3] and Bharadwaj[21] have demonstrated that the M−R binding interaction should be greater than M−F interaction to have efficient disruption of PET communication between the donor and acceptor and hence significant fluorescence recovery of the fluorophore upon binding of metal ions. Present data, in the

Table 5. Decay Parameters and Average Lifetime of DPN in the Absence and Presence of Cu^{2+}

Cu^{2+} conc. ($\times 10^{-6}$ M)	a_1[b]	τ_1 (ns)[a]	a_2[b]	τ_2(ns)[a]	τ_{avg} (ns)[a]	χ^2
0.0	0.98	0.87	0.02	9.28	1.01	0.98
0.67	0.95	1.23	0.05	8.40	1.59	1.15
2.00	0.92	1.18	0.08	8.33	1.81	1.18
3.33	0.86	1.10	0.14	7.77	2.01	1.22
4.67	0.78	1.08	0.22	7.16	2.81	1.12
6.00	0.72	1.23	0.28	6.49	2.72	1.05
7.45	0.66	0.97	0.34	5.50	2.50	1.02

[a]Lifetimes τ_1, τ_2, and τ_{avg} are given in nanoseconds. [b]$a_1$and a_2 are pre-exponential factors, and χ^2 are the goodness-of-fit parameters.

case of Cu^{2+} binding, indicates that even though the disruption of PET takes place, quenching of fluorescence of the parent fluorophore due to the M−F interaction is quite significant. As a result, fluorescence recovery due to disruption of the PET process upon Cu^{2+} binding is not observed completely. We have also performed global analysis (Table S1, Supporting Information) of the fluorescence decay profiles of free DPN and DPN in the presence of metal ions. The binding constant value calculated from the steady-state emission measurements for Zn^{2+} is 1.284 × 10^4 M^{-1} (Figure S11, Supporting Information). This value is found to be very similar to the binding constant value (1.02 × 10^4 M^{-1}) estimated from the decay parameters that are obtained by the global fitting of the lifetime data (Figure S12, Supporting Information). This observation is interesting in a sense that it also provides evidence in favor of the fact that recovery of fluorescence is related to disruption of the PET process upon metal ion binding.

In order to confirm the binding site of metal ions, a ^{1}H NMR study of DPN in the absence and presence of metal ions has been carried out. It has been observed that the NMR peak corresponding to the six dimethyl protons of the dimethyl amino group of the dansylamide moiety undergoes a downfield shift from 2.76 to 2.78 ppm upon addition of Zn^{2+} to DPN (Figure S13, Supporting Information). This shift of the dimethyl protons is expected as the binding of metal ions to the dimethylamine moiety causes a deshielding of the dimethyl protons and thus a downfield shift in the proton NMR signal. The behavior and position of other peaks in the spectrum remain almost the same before and after the addition of the metal salt (Figure S13, Supporting Information). The observation clearly indicates that only the *N*,*N*-dimethyl group of DPN is involved in a binding interaction with Zn^{2+} (Figure S13, Supporting Information). Interestingly, with the addition of Cu^{2+} ions to the solution of DPN, a downfield shift ($\Delta\delta$ = 0.015) for the N−H proton of the sulfonamide group of DPN is observed, whereas the peaks corresponding to the N−CH_3 protons showed a shift of $\Delta\delta$ = 0.022 (Figure S14, Supporting Information). The observation indicates that Cu^{2+} ions are involved in binding interactions with both the *N*,*N*-dimethyl group as well as the sulfonamide group of the dansyl moiety. Significant broadening of the aromatic protons is observed with the further addition of Cu^{2+} ions due to the paramagnetic nature of the copper ion.

3.5. Theoretical Calculations. Theoretical (DFT) calculations have also been carried out to gain a better understanding of the binding interactions between the metal ions and DPN. We have modeled and investigated the interaction of Zn^{2+},

dx.doi.org/10.1021/jp504631n | J. Phys. Chem. B 2014, 118, 9926−9937

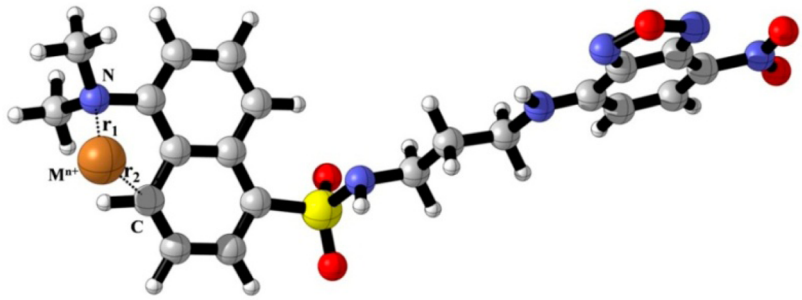

Figure 9. Mode of interaction of M^{n+} ions with DPN in DPN···M^{n+} complexes.

Cu^{2+}, Pb^{2+}, and Cd^{2+} with DPN to understand the nature of binding of transition-metal cations with the receptor. The geometry of DPN···M^{n+} complexes is shown in Figure 9, and their structural features and interaction energies are given in Table 6. It has been found that the metal ions bind to the receptor through the nitrogen atom of the dimethylamine group and an sp^2 carbon atom in the arene ring, as shown in Figure 9. Cu^{2+} binds with the highest binding energy (ΔE_{int} = −306.8 kcal/mol), followed by Zn^{2+}, Cd^{2+}, and Pb^{2+}.

Table 6. Structural Parameters and Cation Binding Energies of DPN···M^{n+} Complexes

DPN···M^{n+} complex	bond distances (Å) r_1	r_2	bond angle (∠CM^{n+}N) (deg)	ΔE_{int} (kcal/mol)
DPN···Zn^{2+}	2.17	2.30	80.30	−199.2
DPN···Cu^{2+}	2.10	2.39	80.12	−306.8
DPN···Pb^{2+}	2.40	2.56	70.48	−110.6
DPN··· Cd^{2+}	2.41	2.54	71.70	−159.9

TDDFT calculations on DPN show the absorption maximum (λ_{max}) at 428.5 nm corresponding to a transition from HOMO−1 to LUMO (95.4%) (Table 7) and a band at 332.0 nm corresponding to a transition from HOMO−1 to LUMO+1 (95.3%). An analysis of the frontier molecular orbitals corresponding to these transitions shows that the absorption maximum arises mainly due to the transitions within the NBD moiety (Figure 10). In the free DPN, along with the 428.5 nm band, a band at 332.0 nm with appreciable oscillator strength has also been observed. Interestingly, in the DPN···Zn^{2+} complex, three new transitions were found at 310.2, 304.9, and 282.3 nm, originating from a number of transitions from HOMO−N orbitals (N = 2, 3, 4) to LUMO and LUMO+1 orbitals. It supports the origin of the new absorption band at around 286 nm that was observed during the addition of Zn^{2+} to DPN solution.

Table 7. Theoretically Calculated Spectroscopic Properties of DPN in ACN

species	absorption maxima (nm)[a]	oscillator strength	transition type	percentage contribution
DPN	428.5	0.332	HOMO−1 → LUMO	95.4%

[a]TD-DFT calculations on DPN at B3LYP/6-311++G(d,p) levels of theory incorporating the implicit solvent model for ACN.

3.6. Cooperative Effect. Finally, in order to investigate whether the binding of one ion affects the binding affinity of other ion (cooperative effect), we have carried out photophysical studies of DPN in the presence of both Zn^{2+} and F^- ions. Representative fluorescence emission spectra from the simultaneous titration experiments are shown in Figures 11 and 12. Stepwise binding constants of anions in the absence and presence of cations and stepwise binding constants of cations in the presence and absence of anions are calculated and presented in Table 8. Stepwise binding constants K_1 and K_2 stand for F^- with DPN in the presence of Zn^{2+}, and K_1' and K_2' stand for Zn^{2+} with DPN in the presence of F^-. The binding constants of ions obtained in the presence of other ions (K_1 and K_2 and K_1' and K_2') were found to be lower compared to those for the ion-free DPN. This decrease in binding (in the presence of another analyte) is also known as negative cooperative effect[60] and indicates the formation of ion pairs during the titration event.[60]

3.7. Fluorescence Microscopy Studies. Further, fluorescence microscopy studies have also revealed that the present DPN system can be employed as an imaging probe in live cells. DPN has been added to the tetrahymena cells at 10 μM final concentrations (the cell density reaches 1 × 10^5 /mL) and incubated for 2 h at 30 °C. The cells have been harvested by centrifugation and used for live cell imaging in a fluorescence microscope. Figure 13 represents the differential interference contrast (DIC) microscopic images and fluorescence microscopic images in a live cell in the absence (Figure 13A) and presence (Figure 13B) of DPN. The result shows that for the present system, DPN is cell-permeable and may be used for live cell imaging studies.

Because it is extremely important for a system to be nontoxic for real time application, we have also carried out the toxicity studies on the present system by employing the same cells. A typical growth curve of tetrahymena in the absence and presence of DPN is shown in Figure S15 (Supporting Information). The data related to growth curve are also provided in Table S2 (Supporting Information). The growth of tetrahymena was found to be similar in the presence or absence of DPN. Hence, DPN is not toxic under the present experimental condition. The response of the present system in the presence of different analytes will be investigated in detail in due course.

4. CONCLUSION

A new nitrobenzoxadizole-based sensor molecule has been synthesized, and its interactions with various metal ions and nonmetal ions have been studied exploiting the PET phenomena. While significant fluorescent enhancement of the emission profile of the system has been observed in the presence of metal ions, a quenching in fluorescence intensity

dx.doi.org/10.1021/jp504631n | J. Phys. Chem. B 2014, 118, 9926−9937

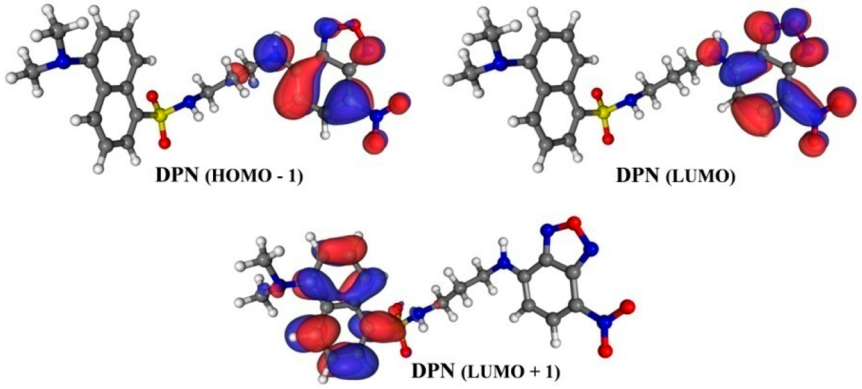

Figure 10. Computed frontier molecular orbitals of DPN.

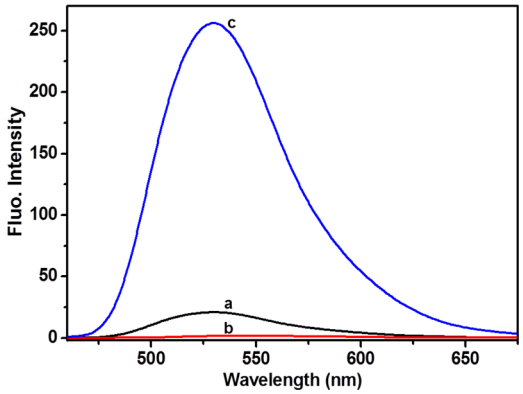

Figure 11. Change in the emission spectrum of DPN (a) upon the addition of fluoride salts (b) and further addition of zinc salts (c).

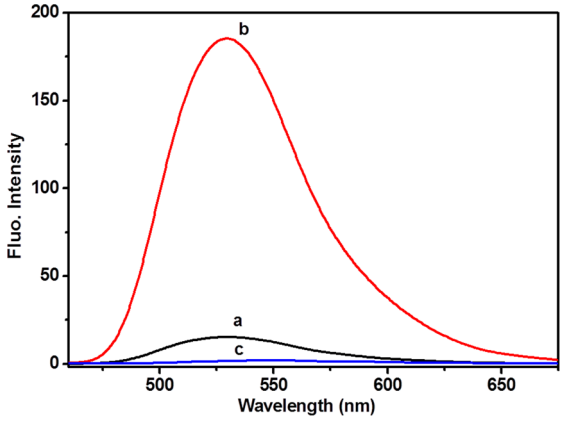

Figure 12. Change in the emission spectrum of DPN (a) upon the addition of zinc salts (b) and further addition of fluoride salts (c).

Table 8. Binding Constants of DPN with F^- in the Presence of Zn^{2+} and of DPN with Zn^{2+} in the Presence of F^-

complexes	binding constant (10^4 M^{-1})
DPN + Zn^{2+}	1.284
DPN + Zn^{2+} (in the presence of F^-)	0.278 (K_1'), 0.035 (K_2')
DPN + F^-	106.2
DPN + F^- (in the presence of Zn^{2+})	0.036 (K_1), 0.0012 (K_2)

has been observed in the presence of anions, allowing the detection of different hosts within a single chemosensor system. The decrease in fluorescence intensity in the presence of anions

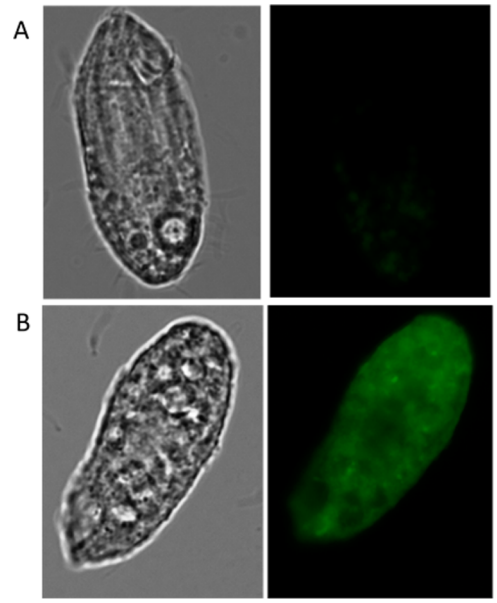

Figure 13. Fluorescence microscopic images of tetrahymena cells treated with (A) 0 and (B) 10 μM DPN. Left panel: DIC microscopy images. Right panel: Fluorescence images.

has been attributed to the hydrogen bonding interaction between the acidic hydrogen atoms of the receptor unit and anions. Compared to other anions studied, the present system is found to be selective for fluoride. FTIR and NMR experiments support the hydrogen bonding interaction between receptors and during the signaling event. The fluorescence enhancement of the present system in the presence of transition-metal ions can be rationalized by considering the disruption of PET communication between the receptor (dimethylamine) and fluorophore (NBD) moiety. Theoretical calculations have also been performed to support the experimental observations. The potential of this system as an imaging probe for fluorescence microscopic studies has also been demonstrated.

■ ASSOCIATED CONTENT

Supporting Information

Figures for the fluorescence response of DPN in the absence and presence of different metal ions, emission spectra of DPN in CH_3CN/H_2O (5:95, v/v) upon progressive addition of $Zn(ClO_4)_2$, Benesi–Hildebrand plot for determination of the binding constant of DPN (1.0×10^{-6} M) with Cu^{2+} ions, NMR

dx.doi.org/10.1021/jp504631n | J. Phys. Chem. B 2014, 118, 9926–9937

spectra with addition of Zn^{2+} and Cu^{2+}, growth of cells, table for growth of the cell in the presence of DPN, and global analysis of lifetime data for DPN in the presence of Zn^{2+}. This material is available free of charge via the Internet at http://pubs.acs.org.

AUTHOR INFORMATION

Corresponding Author

*Email: moloysarkar@gmail.com. Phone: +91-674-2304037. Fax: +91-674-2302436.

Present Address

[§]A.N.: Department of Spectroscopy, Indian Association for the Cultivation of Science, Kolkata 700032 (India).

Notes

The authors declare no competing financial interest.

ACKNOWLEDGMENTS

M.S. thanks the National Institute of Science Education and Research (NISER), Bhubaneswar for funding. A.K.B. is thankful to the Department of Science and Technology (DST), New Delhi for providing the inspired fellowship. S.K.D. is indebted to the Council of Scientific and Industrial Research (CSIR), New Delhi for awarding a fellowship to them. D.M. and P.K.S. are thankful to NISER, Bhubaneswar for the fellowship awarded to them.

REFERENCES

(1) Spichiger-Keller, U. E. *Chemical Sensors and Biosensors for Medical and Biological Applications*; Wiley-VCH: Weinheim, Germany, 1998.

(2) Czarnik, A. W. *Fluorescent Chemosensors for Ion and Molecule Recognition*; American Chemical Society: Washington, DC, 1992.

(3) de Silva, A. P.; Gunaratne, H. Q. N.; Gunnlaugsson, T.; Huxley, A. J. M.; McCoy, C. P.; Rice, J. E. Signaling Recognition Events with Fluorescent Sensors and Switches. *Chem. Rev.* **1997**, *97*, 1515−1566.

(4) Rurack, K. Flipping the Light Switch 'ON' — The Design of Sensor Molecules that Show Cation-Induced Fluorescence Enhancement with Heavy and Transition Metal Ions. *Spectrochim. Acta, Part A* **2001**, *57*, 2161−2195.

(5) Martínez-Máñez, R.; Sancenon, F. Fluorogenic and Chromogenic Chemosensors and Reagents for Anions. *Chem. Rev.* **2003**, *103*, 4419−4476.

(6) Suksai, C.; Tuntulani, T. Chromogenic Anion Sensors. *Chem. Soc. Rev.* **2003**, *32*, 192−202.

(7) Beer, P. D.; Gale, P. A. Anion Recognition and Sensing: The State of the Art and Future Perspectives. *Angew. Chem.* **2001**, *113*, 502−532; *Angew. Chem., Int. Ed.* **2001**, *40*, 486−516.

(8) Gunnlaugsson, T.; Kruger, P. E.; Lee, T. C.; Parkesh, R.; Peffer, F. M.; Hussey, G. M. Dual Responsive Chemosensors for Anions: The Combination of Fluorescent PET (Photoinduced Electron Transfer) and Colorimetric Chemosensors in a Single Molecule. *Tetrahedron Lett.* **2003**, *44*, 6575−6578.

(9) Amendola, V.; Esteban-Gomez, D.; Fabbbrizzi, L.; Lecchelli, M. What Anions Do to N−H-Containing Receptors. *Acc. Chem. Res.* **2006**, *39*, 343−383.

(10) Pérez, J.; Riera, L. Stable Metal−Organic Complexes as Anion Hosts. *Chem. Soc. Rev.* **2008**, *37*, 2658−2667.

(11) Gale, P. A.; Quesada, R. Anion Coordination and Anion-Templated Assembly: Highlights from 2002 to 2004. *Coord. Chem. Rev.* **2006**, *250*, 3219−3244.

(12) Li, A. F.; Wang, J. H.; Wang, F.; Jiang, Y. B. Anion Complexation and Sensing Using Modified Urea and Thiourea-Based Receptors. *Chem. Soc. Rev.* **2010**, *39*, 3729−3745.

(13) Murthy, P. S. Molecular Handshake: Recognition through Weak Noncovalent Interactions. *J. Chem. Educ.* **2006**, *83*, 1010−1013.

(14) Banthia, S.; Samanta, A. A New Strategy for Ratiometric Fluorescence Detection of Transition Metal Ions. *J. Phys. Chem. B* **2006**, *110*, 6437−6440.

(15) Karuppannan, S.; Chambron, J. C. Supramolecular Chemical Sensors Based on Pyrene Monomer−Excimer Dual Luminescence. *Chem.—Asian J.* **2011**, *6*, 964−984.

(16) Arunkumar, E.; Ajayaghosh, A.; Daub, J. Selective Calcium Ion Sensing with a Bichromophoric Squaraine Foldamer. *J. Am. Chem. Soc.* **2005**, *127*, 3156−3164.

(17) Ajayaghosh, A.; Carol, P.; Sreejith, S. A Ratiometric Fluorescence Probe for Selective Visual Sensing of Zn^{2+}. *J. Am. Chem. Soc.* **2005**, *127*, 14962−14963.

(18) Sreejith, S.; Divya, K. P.; Manojkumar, T. K.; Ajayaghosh, A. Multiple Analyte Response and Molecular Logic Operations by Excited-State Charge-Transfer Modulation in a Bipyridine Integrated Fluorophore. *Chem.—Asian J.* **2011**, *6*, 430−437.

(19) Sreenivasu, V. V.; Nehra, A.; Hinge, V. K.; Rao, C. P. Triazole Linked Picolylimine Conjugate of Calix[6]arene as a Sequential Sensor for La^{3+} Followed by F^-. *Org. Lett.* **2012**, *14*, 2968−2971.

(20) Lakowicz, J. R. *Principles of Fluorescence Spectroscopy*; Kluwer/Plenum: New York, 1999.

(21) Das, G.; Bharadwaj, P. K.; Roy, M. B.; Ghosh, S. Transition Metal Cryptate—Enhanced Fluorescence in a Trianthroyl Cryptand: Effect of Spacer on the Photoinduced Electron Transfer Process. *J. Photochem. Photobiol., A* **2000**, *135*, 7−11.

(22) Sauer, M. Single-Molecule-Sensitive Fluorescent Sensors Based on Photoinduced Intramolecular Charge Transfer. *Angew. Chem.* **2003**, *115*, 1834−1837; *Angew. Chem., Int. Ed.* **2003**, *42*, 1790−1793.

(23) Ahmed, N.; Suresh, V.; Shirinfar, B.; Geronimo, I.; Bist, A.; Hwang, I.-C.; Kim, K. S. Fluorogenic Sensing of $CH_3CO_2^-$ and $H_2PO_4^-$ by Ditopic Receptor through Conformational Change. *Org. Biomol. Chem.* **2012**, *10*, 2094−2100.

(24) Cametti, M.; Nissinen, M.; Cort, A. D.; Mandolini, L.; Rissanen, K. Ion Pair Recognition of Quaternary Ammonium and Iminium Salts by Uranyl−Salophen Compounds in Solution and in the Solid State. *J. Am. Chem. Soc.* **2007**, *129*, 3641−3648.

(25) He, X.; Wing-Wah Yam, V. Design, Synthesis, Photophysics, and Ion-Binding Studies of a Ditopic Receptor Based on Gold(I) Phosphine Thiolate Complex Functionalized with Crown Ether and Urea Binding Units. *Inorg. Chem.* **2010**, *49*, 2273−2279.

(26) Reetz, M. T.; Niemeyer, C. M.; Harms, K. Heterotopic Host Molecules for Binding Two Different Guests. *Angew. Chem.* **1991**, *103*, 1517−1519; *Angew. Chem., Int. Ed. Engl.* **1991**, *30*, 1474−1476.

(27) Turner, D. R.; Spencer, E. C.; Howard, J. A. K.; Tocherb, D. A.; Steed, J. W. A Modular, Self-Assembled, Separated Ion Pair Binding System. *Chem. Commun.* **2004**, 1352−1353.

(28) Shukla, R.; Kida, T.; Smith, B. D. Effect of Competing Alkali Metal Cations on Neutral Host's Anion Binding Ability. *Org. Lett.* **2000**, *2*, 3099−3102.

(29) Jose, D. A.; Kumar, D. K.; Ganguly, B.; Das, A. Efficient and Simple Colorimetric Fluoride Ion Sensor Based on Receptors Having Urea and Thiourea Binding Sites. *Org. Lett.* **2004**, *6*, 3445−3448.

(30) Ghosh, T.; Maiya, B. G.; Wong, M. W. Fluoride Ion Receptors Based on Dipyrrolyl Derivatives Bearing Electron-Withdrawing Groups: Synthesis, Optical and Electrochemical Sensing, and Computational Studies. *J. Phys. Chem. A* **2004**, *108*, 11249−11259.

(31) Zienau, J.; Kussmann, J.; Koziol, F.; Ochsenfeld, C. Molecular Recognition in Molecular Tweezers Systems: Quantum-Chemical Calculation of NMR Chemical Shifts. *Phys. Chem. Chem. Phys.* **2007**, *9*, 4552−4562.

(32) Das, S. K.; Misra, S. S.; Sahu, P. K.; Nijamudheen, A.; Mohan, V.; Sarkar, M. Photophysical and Density Functional Studies on the Interaction of a New Nitrobenzoxadiazole Derivative with Anions. *Chem. Phys. Lett.* **2012**, *546*, 90−95.

(33) Sarkar, M.; Samanta, A. Photophysical and Density Functional Studies of the Interaction of a Flavone Derivative with the Halides. *J. Phys. Chem. B* **2007**, *111*, 7027−7033.

(34) Wong, B. M. Noncovalent Interactions in Supramolecular Complexes: A Study on Corannulene and the Double Concave Buckycatcher. *J. Comput. Chem.* **2009**, *30*, 51−56.
(35) Das, S. K.; Patra, A. S.; Jose, D.; Sarkar, M. Investigating the Interaction of A Nitrobenzoxadiazole Derivative with Metal Ions: Photophysical and Theoretical (DFT) Study. *Chem. Phys. Lett.* **2012**, *528*, 11−15.
(36) Mohan, V.; Nijamudheen, A.; Das, S. K.; Sahu, P. K.; Kar, U. P.; Rahaman, A.; Sarkar, M. Ion Interactions with a New Ditopic Naphthalimide-Based Receptor: A Photophysical, NMR and Theoretical (DFT) Study. *ChemPhysChem* **2012**, *13*, 3882−3892.
(37) Ramachandram, B.; Samanta, A. Transition Metal Ion Induced Fluorescence Enhancement of 4-(*N*,*N*-Dimethylethylenediamino)-7-nitrobenz-2-oxa-1,3-diazole. *J. Phys. Chem. B* **1998**, *102*, 10579−10587.
(38) Jisha, V. S.; Thomas, A. J.; Ramaiah, D. Fluorescence Ratiometric Selective Recognition of Cu^{2+} Ions by Dansyl−Naphthalimide Dyads. *J. Org. Chem.* **2009**, *74*, 6667.
(39) Abad, S.; Kluciar, M.; Miranda, M. A.; Pischel, U. Proton-Induced Fluorescence Switching in Novel Naphthalimide−Dansylamide Dyads. *J. Org. Chem.* **2005**, *70*, 10565.
(40) Haldar, S.; Chattopadhyay, A. Application of NBD-Labeled Lipids in Membrane and Cell Biology. *Springer Ser. Fluoresc.* **2013**, *13*, 37−50.
(41) El-Hay, A.; Soad, S.; Colyer, C. L.; Hassan, W. S.; Shalaby, A. Utility of 7-Nitrobenzofurazan (NBD-Cl) for the Spectrophotometric and Spectrofluorometric Determination of Several Antihistamine and Antihypertensive Drugs. *J. AOAC Int.* **2013**, *96*, 968−975.
(42) Robalo, J. R.; Prates, R. J. P.; Loura, L. M. S. NBD-Labeled Cholesterol Analogues in Phospholipid Bilayers: Insights from Molecular Dynamics. *J. Phys. Chem. B* **2013**, *117*, 13731−13742.
(43) Perrin, D. D.; Armarego, W. L. F.; Perrin, D. R. *Purification of Laboratory Chemicals*; Pergamon: New York, 1980.
(44) Crosby, G. A.; Demas, J. N. Measurement of Photoluminescence Quantum Yields. Review. *J. Phys. Chem.* **1971**, *75*, 991−1024.
(45) Rechthaler, K.; Köhler, G. Excited State Properties and Deactivation Pathways of 7-Aminocoumarins. *Chem. Phys.* **1994**, *189*, 99−116.
(46) Zhao, Y.; Schultz, N. E.; Truhlar, D. G. Design of Density Functionals by Combining the Method of Constraint Satisfaction with Parametrization for Thermochemistry, Thermochemical Kinetics, and Noncovalent Interactions. *J. Chem. Theory Comput.* **2006**, *2*, 364−382.
(47) Zhao, Y.; Truhlar, D. G. The M06 Suite of Density Functionals for Main Group Thermochemistry, Thermochemical Kinetics, Noncovalent Interactions, Excited States, and Transition Elements: Two New Functionals and Systematic Testing of Four M06-Class Functionals and 12 Other Functional. *Theor. Chem. Acc.* **2008**, *120*, 215−241.
(48) Hariharan, P. C.; Pople, J. A. The Influence of Polarization Functions on Molecular Orbital Hydrogenation Energies. *Theor. Chim. Acta* **1973**, *28*, 213−222.
(49) Hay, P. J.; Wadt, W. R. *Ab Initio* Effective Core Potentials for Molecular Calculations. Potentials for K to Au Including the Outermost Core Orbitals. *J. Chem. Phys.* **1985**, *82*, 299−310.
(50) Roy, L. E.; Hay, P. J.; Martin, R. L. Revised Basis Sets for the LANL Effective Core Potentials. *J. Chem. Theory Comput.* **2008**, *4*, 1029−1031.
(51) Simon, S.; Duran, M.; Dannenberg, J. J. How Does Basis Set Superposition Error Change the Potential Surfaces for Hydrogen-Bonded Dimers? *J. Chem. Phys.* **1996**, *105*, 11024−11031.
(52) Becke, D. A. Density-Functional Thermochemistry. III. The Role of Exact Exchange. *J. Chem. Phys.* **1993**, *98*, 5648.
(53) Marenich, A. V.; Cramer, C. J.; Truhlar, D. G. Universal Solvation Model Based on Solute Electron Density and on a Continuum Model of the Solvent Defined by the Bulk Dielectric Constant and Atomic Surface Tensions. *J. Phys. Chem. B* **2009**, *113*, 6378−6396.
(54) Frisch, M. J.; et al. *Gaussian 09*, revision 09.A0; Gaussian, Inc.: Wallingford, CT, 2009.
(55) Benesi, M. L.; Hildebrand, J. H. A Spectrophotometric Investigation of the Interaction of Iodine with Aromatic Hydrocarbons. *J. Am. Chem. Soc.* **1949**, *71*, 2703−2707.
(56) Métivier, R.; Leray, I.; Valeur, B. Photophysics of Calixarenes Bearing Two or Four Dansyl Fluorophores: Charge, Proton and Energy Transfers. *Photochem. Photobiol. Sci.* **2004**, *3*, 374−380.
(57) Cui, S.-C.; Tachikawa, T.; Fujitsuka, M.; Majima, T. Solvent-Polarity Dependence of Electron-Transfer Kinetics in a CdSe/ZnS Quantum Dot−Pyromellitimide Conjugate. *J. Phys. Chem. B* **2010**, *114*, 1217−1225.
(58) Guy, J.; Karine, C.; Dufresne, S.; Michnick, S. W.; Skene, W. G.; Keillor, J. W. Convergent Preparation and Photophysical Characterization of Dimaleimide Dansyl Fluorogens: Elucidation of the Maleimide Fluorescence Quenching Mechanism. *J. Am. Chem. Soc.* **2007**, *129*, 11969−11977.
(59) Shankar, B. H.; Ramaiah, D. Dansyl—Naphthalimide Dyads as Molecular Probes: Effect of Spacer Group on Metal Ion Binding Properties. *J. Phys. Chem. B* **2011**, *115*, 13292−13299.
(60) Shukla, R.; Kida, T.; Smith, B. D. Effect of Competing Alkali Metal Cations on Neutral Host's Anion Binding Ability. *Org. Lett.* **2000**, *2*, 3099−3102.